

Insights into the Reaction Mechanism of the Prolyl–Acyl Carrier Protein Oxidase Involved in Anatoxin-a and Homoanatoxin-a Biosynthesis

Stéphane Mann,^{†,‡} Bérangère Lombard,^{||} Damarys Loew,^{||} Annick Méjean,^{†,‡,§} and Olivier Ploux^{*,†,‡}

[†]Laboratoire Charles Friedel, Chimie ParisTech, ENSCP, 11 rue Pierre et Marie Curie, 75231 Paris Cedex 05, France

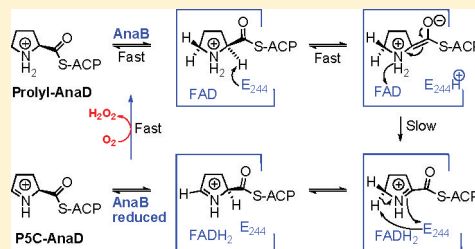
[‡]CNRS, UMR 7223, 75005 Paris, France

[§]Université Paris Diderot-Paris 7, 75013 Paris, France

^{||}Laboratory of Proteomic Mass Spectrometry, Centre de Recherche, Institut Curie, 26 rue d'Ulm 75248, Paris Cedex 05, France

S Supporting Information

ABSTRACT: Anatoxin-a and homoanatoxin-a are two potent cyanobacterial neurotoxins. We recently reported the identification of the gene cluster responsible for the biosynthesis of these toxins as well as the in-vitro reconstitution of the first steps of this biosynthesis. We now report experimental evidence supporting the proposed reaction mechanism of AnaB, a flavoprotein homologous to acyl-CoA dehydrogenase. AnaB catalyzes the two-electron oxidation of prolyl-AnaD, which is proline linked to the acyl carrier protein holo-AnaD, to dehydroprolyl-AnaD using oxygen as the second substrate. AnaB is thus an oxidase. By using liquid chromatography coupled to tandem mass spectrometry (LC-MS/MS), we have identified and characterized dehydroprolyl-AnaD, the AnaB product. We estimated an apparent catalytic constant of 1 min⁻¹ for AnaB catalysis. We synthesized several deuterium-labeled prolines and enzymatically transformed them into their corresponding prolyl-AnaD. These deuterium-labeled prolyl-AnaDs were oxidized in the presence of AnaB, and the deuterium labeling in the remaining substrate and in the product was determined by LC-MS/MS. The data supported a reaction mechanism starting with a rapid enolization followed by a slow oxidation to give the conjugated imine, which in turn was isomerized to pyrroline-5-carboxyl-AnaD. We also showed that *cis*- and *trans*-4-fluoro-L-prolyl-AnaD and 3,4-dehydro-L-prolyl-AnaD were transformed into pyrrole-2-carboxyl-AnaD by AnaB. Thus, the 4-fluoro-analogues experienced a β -elimination supporting the AnaB-catalyzed aza-allylic isomerization. We identified by sequence alignment the AnaB active site base, Glu244. We produced, purified, and characterized the E244A AnaB mutant, which is inactive, supporting the catalytic role of E244 as a base.



Cyanobacteria produce a wide range of secondary metabolites including toxins to human and animals.¹ These oxygenic photosynthetic prokaryotes can be found in almost every terrestrial or aquatic environment and thus pose a threat to human and animal health. Indeed, cases of animal death and human intoxication, due to cyanobacterial toxin exposure, are regularly reported in different places around the world.^{2–7} For instance, anatoxin-a and homoanatoxin-a, two cyanobacterial neurotoxins, provoke the rapid death of animals by acute asphyxia, when ingested, because these alkaloids are potent agonists of the nicotinic acetylcholine receptor.⁸ We have recently reported the identification of the gene cluster responsible for the biosynthesis of these toxins in the cyanobacterium *Oscillatoria* sp. PCC 6506 (PCC stands for Pasteur culture collection of cyanobacteria) and proposed an original biosynthetic scheme for these alkaloids (Scheme 1).⁹ The identification of the *ana* biosynthetic genes was an important step because it provided a simple way to detect in water the presence of anatoxin-a producing cyanobacteria by specific PCR amplifications.^{10–12}

However, the discovery of the *ana* genes and of the biosynthetic route leading to anatoxin-a and homoanatoxin-a revealed some interesting enzymatic steps, as shown in Scheme 1. We proposed that proline is loaded on AnaD, an acyl carrier protein (ACP), and oxidized to (S)-1-pyrroline-5-carboxyl-AnaD (P5C-AnaD). This starter would then be transferred to the polyketide synthase (PKS) AnaE for elongation. The second PKS, AnaF, would then add another acetate unit and catalyze a Mannich-type cyclization step to form anatoxin acid linked to the ACP module of AnaF. The third PKS, AnaG, would catalyze the formation of the β -oxo-thioester precursor of anatoxin-a or, if a methylation had occurred on AnaG, that of homoanatoxin-a. Hydrolysis of the β -oxo-thioester and decarboxylation of the acid, to give the corresponding toxin, would be catalyzed by the thioesterase, AnaA. We have recently reconstituted in vitro the first steps of this pathway and showed that AnaC is indeed a proline specific adenylation protein and

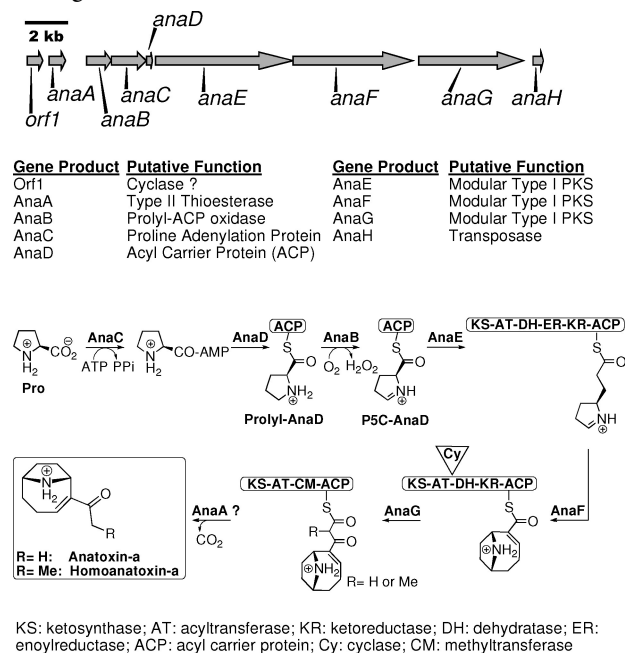
Received: June 9, 2011

Revised: July 22, 2011

Published: July 25, 2011



Scheme 1. The *ana* Gene Cluster Responsible for the Biosynthesis of Anatoxin-a and Homoanatoxin-a in Cyanobacteria and the Postulated Biosynthetic Route Leading to These Neurotoxins



provided initial experimental evidence supporting the formation of dehydropyrol-AnaD from prolyl-AnaD by the flavoprotein AnaB.¹³ We also noted that these steps leading to P5C-AnaD were reminiscent of those involved in the formation of pyrrole-2-carboxyl-ACP, the starter of a number of biosyntheses of pyrrole containing secondary metabolites.^{14–26} However, AnaB is unique among these enzymes because it catalyzes a two-electron oxidation reaction rather than a four-electron oxidation as its homologues.

We now report the complete identification and characterization, by high performance liquid chromatography (HPLC) and by liquid chromatography coupled to tandem mass spectrometry (LC-MS/MS), of dehydropyrol-AnaD, the AnaB product. Using diverse deuterium-labeled prolines as well as 4-fluoro-L-prolines and 3,4-dehydro-L-proline, we have studied the reaction mechanism of this oxidation step. We provide new evidence supporting a reaction mechanism, for this flavoprotein, involving several steps to give P5C-AnaD as the product. We have also identified, by site-directed mutagenesis, the putative active site base of AnaB and showed that this enzyme uses oxygen as the second substrate. AnaB is thus a close homologue of acyl-CoA dehydrogenase (ACAD) like the human isovaleryl-CoA dehydrogenase (hIVD), in terms of sequence and reaction mechanism, but is rather an oxidase than a dehydrogenase.

EXPERIMENTAL PROCEDURES

General. Alignments of protein sequences were performed using the Clustal X software.²⁷ Chemicals and biochemicals were purchased from Sigma-Aldrich. HPLC was run on a Hewlett-Packard 1050 series apparatus equipped with a Jupiter 5 μ m C18 300 Å Phenomenex column. Elutions were performed using a linear gradient (from 60% to 80% (v/v) in 20 min) of methanol in aqueous 0.1% trifluoroacetic acid (TFA) at 1 mL/min, and the detector was set at 210 nm. UV–

vis spectra and absorbance measurements were recorded on an UVikon 930 Kontron spectrophotometer. NMR spectra were recorded at the ENSCP NMR laboratory. Protein purifications were achieved using an integrated protein purification system (AKTApurifier, GE Healthcare). PCR amplifications and electrophoretic separations (agarose and acrylamide) were run as already described.⁹ Protein concentrations were estimated by using the Bradford colorimetric assay (BioRad).²⁸ Recombinant histidine-tagged, apo-AnaD, holo-AnaD, AnaC, and wild-type AnaB were obtained as previously described.^{9,13}

Synthesis of Deuterium-Labeled Proline. The following synthesis have been adapted from previous works.^{29–32}

(\pm)-[2-²H]-2-Carboxypyrrolidinium Chloride (1). L-Proline (265 mg, 2.3 mmol) was dissolved in D₂O (1.5 mL) to substitute exchangeable hydrogen atoms by deuterium, and the solution was concentrated under vacuum. The residue was placed under an argon atmosphere, and pyridoxal-5'-phosphate (PLP, 53 mg, 0.2 mmol) was added. Then the mixture was dissolved in a solution of NaOD prepared from sodium (265 mg, 11.5 mmol) and D₂O (2 mL) and refluxed under argon for 8 h. The resulting solution was acidified to pH 1 with aqueous 1 M HCl and loaded on a TEMEX 50W-x8 column, which was eluted with a gradient of aqueous HCl (from 0 to 1 M). The fractions containing proline were concentrated, and the hydrochloride salt of deuterium-labeled proline was isolated as white crystals; mp 158 °C, lit. 156 °C.³⁰ Because the deuterium incorporation after this process was only 58%, as measured by integrating the NMR signal of the C2–H proton, the reaction was repeated twice until incorporation of deuterium at that position reached a value of 97%. ¹H NMR (400 MHz, D₂O): δ 2.05 (2H, m, CH₂CH₂N), 2.16 (1H, m, CH₂CHCO), 2.42 (1H, m, CH₂CHCO), 3.40 (2H, m, CH₂N), 4.45 (0.03H, m, CH). ¹³C NMR (75 MHz, D₂O): δ 23.3 (CH₂CH₂N), 28.2 (CH₂CHCO), 46.2 (CH₂N), 59.3 (CD, t), 171.9 (CO).

(2S)-5-(Piperidine-1-carbonyl)pyrrolidin-2-one (2). A mixture of L-pyrroglutamic acid (1 g, 7.7 mmol), 1-hydroxybenzotriazole (HOBT, 1 g, 7.7 mmol), and *N,N'*-dicyclohexylcarbodiimide (DCC, 1.6 g, 7.7 mmol) in tetrahydrofuran (THF, 25 mL) was stirred 10 min at room temperature under an argon atmosphere. Piperidine (760 μ L, 7.7 mmol) was then added dropwise, and the solution was stirred for 4 h. After concentrating the solution under vacuum, the crude mixture was separated by flash chromatography (CH₂Cl₂/ethanol: 195/5 to 180/20, v/v) to give compound 2 as a colorless oil (1.4 g, 95% yield). ¹H NMR (300 MHz, CDCl₃): δ 1.52–1.64 (6H, m, CH₂CH₂CH₂N), 2.02–2.12 (1H, m, CH₂CH₂CO), 2.28–2.48 (3H, m, CH₂CH₂CO), 3.31–3.62 (4H, m, CH₂N), 4.48 (1H, t, *J* = 8.0 Hz, CHCO), 6.82 (1H, broad, NH). ¹³C NMR (75 MHz, CDCl₃): δ 24.3 (CH₂CH₂CO), 25.3 (CH₂CH₂N), 26.3 (CH₂CH₂CH₂N), 29.5 (CH₂CO), 43.3 and 46.0 (CH₂N), 54.2 (CHN), 169.5 (CO), 178.3 (CO).

(2S)-1-(tert-Butoxycarbonyl)-5-(piperidine-1-carbonyl)-pyrrolidin-2-one (3). A solution composed of 2 (600 mg, 3 mmol), di-*tert*-butyl dicarbonate (Boc₂O, 1.3 g, 6 mmol), 4-(dimethylamino)pyridine (DMAP, 37 mg, 0.3 mmol), and dry acetonitrile (7 mL) under an argon atmosphere was stirred overnight at room temperature. After concentration under vacuum, the crude mixture was purified by flash chromatography (cyclohexane/ethyl acetate: 5/5 to 0/1, v/v). The *tert*-butoxycarbonyl (Boc) derivative 3 was isolated as a white powder (638 mg, 72% yield). ¹H NMR (300 MHz, CDCl₃): δ

1.44 (9H, s, CH₃), 1.54–1.64 (6H, m, CH₂), 1.79–1.84 (1H, m, CH₂CH₂CO), 2.14–2.28 (1H, m, CH₂CH₂CO), 2.35–2.44 (1H, m, CH₂CO), 2.56–2.69 (1H, m, CH₂CO), 3.36–3.48 (3H, m, CH₂N), 3.60–3.68 (1H, m, CH₂N), 4.91 (1H, dd, *J* = 1.5 Hz and *J* = 9.0 Hz, CHN). ¹³C NMR (75 MHz, CDCl₃): δ 21.6 (CH₂CH₂CO), 24.3 (CH₂CH₂CH₂N), 25.5 and 26.4 (CH₂CH₂N), 27.9 (C(CH₃)₃), 31.2 (CH₂CO), 43.3 and 46.1 (CH₂N), 56.6 (CHN), 82.2 (C(CH₃)₃), 149.5 (CO), 168.5 (CO), 173.9 (CO).

(2*S*)-1-(*tert*-Butoxycarbonyl)-2-(piperidine-1-carbonyl)-[5,5-²H₂]-pyrrolidine (**4**). A solution of iodine (305 mg, 1.2 mmol) in dry THF (2 mL) was slowly added (in 3 h) dropwise to a solution of **3** (296 mg, 1 mmol) in dry THF (2 mL) in the presence of NaBD₄ (84 mg, 2 mmol, 97% deuterium labeling) at –12 °C, and the temperature was maintained constant over the experiment. The reaction was stopped at –5 °C by adding ethanol (1 mL), and the mixture was diluted with CH₂Cl₂ (5 mL) and brine (1 mL). The organic layer was separated, dried over MgSO₄, concentrated under vacuum, and separated by flash chromatography (cyclohexane/ethyl acetate: 7/1 to 0/1, v/v). The pyrrolidine **4** was isolated as a yellow oil (119 mg, 42% yield). NMR spectra showed the presence of two rotamers in a 1/1 ratio. Estimated deuterium labeling at position C5 = 90%. ¹H NMR (300 MHz, CDCl₃): δ 1.36 and 1.41 (9H, s, CH₃), 1.50–1.70 (6H, m, CH₂), 1.78–1.82 (2H, m, CH₂), 1.86–1.99 (1H, m, CH₂CHCO), 2.04–2.19 (1H, m, CH₂CHCO), 3.30–3.70 (4.2H, m, CH₂N), 4.48 and 4.63 (1H, dd, *J* = 2.6 and 8.3 Hz, CHCO). ¹³C NMR (75 MHz, CDCl₃): δ 23.2 and 23.8 (CH₂CH₂CO), 24.5 (CH₂CH₂CH₂N), 25.7 and 26.4 (CH₂CH₂N), 28.4 and 28.5 (C(CH₃)₃), 29.8 and 30.5 (CH₂CO), 43.1 and 46.2 (CH₂N), 56.5 and 56.9 (CHN), 79.2 (C(CH₃)₃), 154.0 and 154.5 (CO), 170.4 and 170.5 (CO).

(2*S*)-[5,5-²H₂]-2-Carboxypyrrolidinium Chloride (**5**). The pyrrolidine **4** was solubilized in a (1/1, v/v) TFA/CH₂Cl₂ solution (3 mL) and stirred for 30 min at room temperature. The solvents were removed by successive dilutions with CH₂Cl₂ and concentrations under vacuum (3 times). The crude product was then solubilized in an aqueous 0.5 M NaOH solution (3 mL) and refluxed overnight. The mixture was acidified to pH 3 with an aqueous 1 M HCl solution and purified on a TEMEX 50W-x8 column that was eluted with an aqueous HCl gradient (from 0 to 1 M). The fractions containing proline were combined and evaporated to afford the hydrochloride salt of the labeled proline **5** (54 mg, 85% yield); mp 60 °C, lit. 115 °C (30); [α]_D²² –33.1° (H₂O, *c* = 2); deuterium labeling at position C5 = 91%. ¹H NMR (300 MHz, D₂O): δ 2.02 (2H, t, *J* = 7.0 Hz, CH₂CD₂), 2.08–2.20 (1H, m, CH₂CH), 2.35–2.47 (1H, m, CH₂CH), 3.35 and 3.40 (0.09H, t, *J* = 7.5 Hz, CHDNH), 4.38 (1H, t, *J* = 7.7 Hz, CHN). ¹³C NMR (75 MHz, D₂O): δ 23.1 and 28.3 (CH₂CH₂), 45.9 (CD₂), 59.6 (CH), 172.0 (CO).

tert-Butyl (2*S*)-5-Oxo-pyrrolidine-2-carboxylate (**6**). A solution of L-pyrogutamic acid (2 g, 15.5 mmol) in *tert*-butyl acetate (8 mL, 60 mmol) and in aqueous 70% w/v HClO₄ (0.5 mL) was stirred under argon for 24 h. The mixture was then poured into a saturated aqueous NaHCO₃ solution (50 mL) and extracted with diethyl ether (4 × 100 mL). The organic layer was then dried over MgSO₄ and concentrated under vacuum to give **6** as a white powder (1.18 g, 31% yield). ¹H NMR (300 MHz, CDCl₃): δ 1.41 (9H, s, CH₃), 2.10 (1H, m, CH₂), 2.31 (2H, m, CH₂), 2.37 (1H, m, CH₂), 4.08 (1H, m,

CH), 6.64 (1H, broad, NH). ¹³C NMR (75 MHz, CDCl₃): δ 24.8 (CH₂), 27.9 (CH₃), 29.4 (CH₂), 56.2 (CHN), 82.3 (C(CH₃)₃), 171.1 (CO), 178.2 (CO).

tert-Butyl (2*S*)-(1-*tert*-Butoxycarbonyl)-5-oxo-pyrrolidine-2-carboxylate (**7**). The ester **6** (1.1 g, 5.9 mmol) was solubilized in THF (23 mL) in the presence of DMAP (55 mg, 0.45 mmol) and Boc₂O (1.96 g, 9 mmol) at 4 °C, under an argon atmosphere. The stirring was maintained overnight, and the temperature was raised to room temperature. Then the mixture was concentrated and purified by flash chromatography (cyclohexane/ethyl acetate: 9/1 to 7/3, v/v) to give the Boc-derivative **7** as a yellow oil, which crystallized (1.6 g, 95% yield). ¹H NMR (300 MHz, CDCl₃): δ 1.49 (9H, s, CH₃), 1.51 (9H, s, CH₃), 1.95–2.05 (1H, m, CH₂), 2.22–2.36 (1H, m, CH₂), 2.42–2.68 (2H, m, CH₂), 4.48 (1H, dd, *J* = 2.6 Hz and *J* = 9.4 Hz, CH). ¹³C NMR (75 MHz, CDCl₃): δ 21.6 (CH₂), 27.9 (CH₃), 31.1 (CH₂), 59.6 (CH), 82.2 and 83.3 (C(CH₃)₃), 149.3 (CO), 170.3 (CO), 173.5 (CO).

tert-Butyl (2*S*)-(1-*tert*-Butoxycarbonyl)-5-hydroxypyrrolidine-2-carboxylate (**8**). A solution of carbamate **7** (1 g, 3.5 mmol) in dry THF (30 mL) was cooled to –78 °C, and 5 mL of a 1 M solution of diisobutylaluminum hydride (DIBAL-H) in dry THF was added dropwise over 10 min. The mixture was maintained under stirring at this temperature for 2 h, and the reaction was quenched by adding a saturated aqueous solution of NaHCO₃. The temperature was slowly increased to room temperature in 20 min. An aqueous solution of 35% w/v H₂O₂ (10 drops) was then added, and stirring was maintained at this temperature for 30 min. The mixture was diluted with CH₂Cl₂ (200 mL), with a saturated aqueous solution of NaHCO₃ (40 mL), and with water (40 mL). The organic layer was extracted with CH₂Cl₂ (2 × 75 mL), and the combined fractions were dried and concentrated over Na₂SO₄. The crude product was then purified by flash chromatography (cyclohexane/ethyl acetate: 9/1 to 7/3, v/v) to yield **8** as a mixture of diastereoisomers and conformers (yellow oil, 950 mg, 95% yield); *R*_f = 0.3 (cyclohexane–AcOEt). ¹H NMR (300 MHz, CDCl₃): δ 1.36, 1.38, 1.41, 1.43 (18H, s, CH₃), 1.74–2.05 (2H, m, CH₂CH₂), 2.10–2.60 (2H, m, CH₂CH₂), 2.75 (1H, broad, OH), 4.05–4.45 (1H, m, CHCO), 5.35–5.58 (1H, m, CHOH). ¹³C NMR (75 MHz, CDCl₃): δ 27.9, 27.94, 28.3, 28.4 (CH₃), 30.9, 31.1, 32.2 (CH₂CH₂), 59.6, 59.9, 60.0 (CHCO), 80.7, 80.9, 81.1 (C(CH₃)₃), 81.9, 82.2, 82.5, 88.3 (CHOH), 154.4 (CO), 171.6 (CO).

tert-Butyl (2*S*,5*S*)-(1-*tert*-Butoxycarbonyl)-[5-²H]-pyrrolidine-2-carboxylate (**9**). A solution of hemiaminal **8** (150 mg, 0.52 mmol) in anhydrous toluene (5 mL) under an argon atmosphere was cooled down to –78 °C, and freshly distilled BF₃–OEt₂ (160 μL, 1.14 mmol) and Bu₃SnD (280 μL, 1.06 mmol, 96% deuterium labeling) were added in two portions at 30 min intervals. The mixture was stirred at this temperature for 4 h. Then, the reaction was quenched by adding saturated aqueous NaHCO₃ (0.5 mL). The mixture was warmed to room temperature, diluted with 10% aqueous NaHCO₃, and extracted with CH₂Cl₂ (3 × 10 mL). The organic layer was dried over Na₂SO₄, concentrated, and purified by flash chromatography (cyclohexane/ethyl acetate: 9/1, v/v). The labeled pyrrolidine **9** was obtained as a colorless oil (20 mg, 15% yield). ¹H NMR (300 MHz, CDCl₃): δ 1.41 and 1.44 (18H, s, CH₃), 1.76–1.96 and 2.10–2.24 (3H + 1H, m, CH₂CH₂), 3.39 and 3.50 (1H, m, CHD), 4.06–4.17 (1H, m, CHCO). ¹³C NMR (75 MHz, CDCl₃): δ 23.3 and 24.1

(CH₂CHCO), 27.9 and 28.0 (CH₃), 29.7 and 30.9 (CH₂CHD), 46.5 (CHD), 58.4 and 59.7 (CHCO), 79.6 and 80.8 (C(CH₃)₃), 154.0 (CO), 172.3 (CO).

(2S,5S)-[5-²H]-2-Carboxypyrrolidinium Chloride (10). Compound **9** (20 mg, 0.073 mmol) was stirred in a (1/1, v/v) TFA/CH₂Cl₂ solution (2 mL) for 20 min at room temperature. After concentration of the mixture, the excess of TFA was removed by successive dilution–concentration cycles with CH₂Cl₂ (three times). The resulting oil was solubilized in aqueous 2 M HCl (2 mL) and refluxed for 3 h. After concentrating under vacuum, the hydrochloride salt of proline **10** was obtained (11 mg, quantitative yield). [α]_D²² –21° (H₂O, c = 1.5). Integration of the ¹H NMR spectrum of **10** showed that the C5-H_{pro}-R and C5-H_{pro}-S integrated for 0.85 and 0.15, respectively. ¹H NMR (400 MHz, D₂O): δ 1.90–1.95 (2H, m, CH₂CHD), 1.99–2.07 (1H, m, CH₂CHCO), 2.26–2.33 (1H, m, CH₂CHCO), 3.25 (0.85H, t, J = 8.0 Hz, (5R)-CHD), 3.30 (0.15H, t, J = 8.0 Hz, (5S)-CHD), 4.25 (1H, t, J = 7.8 Hz, CHCO). ¹³C NMR (75 MHz, D₂O): δ 23.2 and 28.2 (CH₂CH₂), 45.9 (t, CHD), 59.6 (CHCO), 172.0 (CO).

Cloning, Expression, and Purification of the Recombinant Histidine-Tagged *Oscillatoria* PCC 6506 E244A AnaB.

The entire plasmid, containing the wild-type *anaB* gene for production of the histidine-tagged recombinant protein,¹³ was PCR-amplified (Phusion polymerase, New England BioLabs) using the following primers (Eurogentec): *anaBPstIF*, 5'-CTA-GCC-GCT-GCA-GTG-GGA-ACA-ATG-GAA-CG-3', containing a silent mutation (bold typed) that creates a unique *PstI* site (underlined), and *anaBE244AR*, 5'-GCC-TGC-AGC-GGC-TAG-AAT-AAA-TCC-CCG-TGC-CCA-CTC-CAT-AC-3', containing a GC clamp (italicized), a single silent mutation (bold typed) that creates a unique *PstI* site (underlined), and a single mutation (bold typed) that creates the E244A amino acid replacement. The overlapping sequence (5'-CTA-GCC-GCT-GCA-G-3') of the two primers contains the unique new *PstI* restriction site (underlined). The resulting 6.4 kb PCR product was subjected to electrophoretic separation on a 0.8% (w/v) agarose gel, and the band was excised and extracted (PCR purification Kit, Promega). After digestion with *PstI* the PCR product was circularized using T4 DNA ligase (Promega), and the ligation product was used to transform chemically competent *E. coli* JM109 cells. Positive clones (lysogeny broth (LB) agar containing 50 μ g/mL of kanamycin) were analyzed and the plasmid purified, and the E244A *anaB* insert sequence was verified by DNA sequencing (GATC Co.). The plasmid pETanaBE244A was used for production of the recombinant E244A AnaB histidine-tagged protein in *E. coli* BL21-CodonPlus (DE3)-RIPL strain (Stratagene), essentially as described for the wild-type enzyme¹³ with slight modifications. Briefly, the resulting strain was grown in LB medium supplemented with chloramphenicol (35 μ g/mL) and kanamycin (50 μ g/mL) at 37 °C with shaking until it reached an absorbance of 1 at 600 nm. The culture medium was then cooled down to 16 °C; isopropyl- β -D-thiogalactopyranoside (IPTG) was then added to a final concentration of 250 μ M, and the culture was left overnight at 16 °C with shaking. The resulting cells were harvested by centrifugation (4000g, at 4 °C for 20 min, Sorval RC5B centrifuge, SLA-3000 rotor) and lysed by sonication (Misonix sonicator 500 W, 3 mm probe, 3 min with 10 s pulses spaced by 20 s cooling periods at 4 °C) in 20 mM Na-phosphate buffer, pH 7.4, 0.5 M NaCl, 20 mM imidazole, 100 μ M FAD. After centrifugation (two runs at

26000g, SS-34 rotor, 15 min) the supernatant was loaded on a 1 mL HisTrap column (GE Healthcare). The desired protein was eluted with a linear gradient of imidazole (20–500 mM) in 20 mM Na-phosphate buffer, pH 7.4, 0.5 M NaCl. Pure fractions of AnaB were pooled, and the protein was desalted and concentrated by ultrafiltration (Amicon Ultra-15 Centrifugal Filter Unit 30k) and stored in 20 mM Tris-HCl buffer, pH 7.4, 20% (v/v) glycerol at –80 °C. A sample of pure recombinant E244A AnaB (30 μ g) was injected and purified by HPLC, under the conditions described above. The single peak at 15.5 min was collected, and the solution was concentrated under vacuum and analyzed by electrospray ionization mass spectrometry (ESI-MS), as already described.¹³ The protein showed an experimental mass of 46 358.4 Da, in agreement with the calculated mass of 46 359.07 Da for the protein lacking the first Met. Recombinant wild-type AnaB, analyzed using the same conditions, showed an experimental mass of 46 417.7 Da for a calculated mass of 46 417.1 Da for the protein lacking the first Met.

Dithionite Reduction of AnaB and Oxidation by Air. A solution of either recombinant histidine-tagged wild-type AnaB (7.9 μ M) or its E244A mutant (12.8 μ M) in 20 mM Tris-HCl buffer, pH 7.7, containing 10% v/v glycerol was introduced in a cuvette fitted with a rubber septum. The electronic absorption spectrum of the solutions was then recorded at room temperature. Then, freshly prepared dithionite (52 mM sodium dithionite aqueous solution) was added to the enzyme solution to a final concentration of 0.52 mM through the septum using a gastight syringe, the solution was gently mixed by manual inverting, and the electronic absorption spectrum was recorded. The solution was then exposed to air and gently mixed by manual inverting, and the electronic absorption spectrum was recorded again.

Preparation of Prolyl-AnaD and Analogues. Prolyl-AnaD was prepared as previously described.^{9,13} The assay consisted (100 μ L total volume) of 100 mM Tris-HCl, pH 7.7, 1 mM tris(2-carboxyethyl)phosphine (TCEP), 10 mM MgCl₂, 5 mM ATP, 5 mM L-proline, 80 μ M holo-AnaD, and 1 μ M AnaC, and the reaction was incubated at 28 °C for 30 min. For preparation of large quantities of prolyl-AnaD the assay was adapted to 2 mL total volume, and the concentration of AnaC was 2 μ M. The prolyl-AnaD was not further purified because of its instability (hydrolysis of the thioester bond) and used as such for oxidation by AnaB. The analogues were produced using the same procedure except that L-proline was replaced by either 10 mM [2-²H]-DL-proline **1** or 5 mM of either [5,5-²H₂]-L-proline **5**, 5-(S)-[5-²H]-L-proline **10**, [2,3,3,4,4,5,5-²H₇]-L-proline (Cambridge Isotope, proline-d₇, 97–98%), 4-(R)-4-fluoro-L-proline (Bachem), 4-(S)-4-fluoro-L-proline (Bachem), or 3,4-dehydro-L-proline (Sigma). The reaction of formation of each prolyl-AnaD analogue was followed by HPLC using the conditions described above to ensure that the conversion was complete. The retention times were the followings: holo-AnaD 19.3 min; prolyl-AnaD and deuterium-labeled analogues 18.3 min; 4-fluoro-prolyl-AnaD 17.2 min; 3,4-dehydro-L-prolyl-AnaD 18.0 min.

AnaB-Catalyzed Oxidation Reaction of Prolyl-AnaD and Analogues. Prolyl-AnaD, prepared as described above, was oxidized in the presence of 10 μ M purified recombinant histidine-tagged wild-type AnaB. The enzyme was directly added to the prolyl-AnaD solution (60 μ M final concentration of prolyl-AnaD, 100 μ L final volume), and the reaction mixture

was incubated for 5 min at 28 °C. The sample was then immediately analyzed by HPLC or frozen at −20 °C for subsequent analysis by HPLC or LC-MS/MS. Dehydroprolyl-AnaD eluted at 18.9 min, slightly after prolyl-AnaD under the HPLC conditions described above. AnaB eluted at 15.5 min. The same procedure was used for all prolyl-AnaD analogues and for control experiments in the absence of AnaB or in the presence of E244A AnaB (10 μM). Oxidized products always eluted slightly after the corresponding reduced substrate, but the peaks overlapped and the separation was not optimized.

Mass Spectrometry Analyses. Prolyl-AnaD, analogues, and AnaB-oxidized products were analyzed using two different strategies. The first one consisted in digesting the samples by trypsin followed by LC-MS/MS analysis as already described.¹³ The mass and isotopic distributions of the ion corresponding to the dephosphorylated phosphopantetheinyl arm with proline (m/z 358.18) or dehydroproline (m/z 356.17) or analogues attached to it were then determined. The second strategy, which allowed rapid analysis to avoid degradation or possible nonenzymatic exchange of deuterium, is based on LC separation of prolyl-AnaD or analogues and its oxidized product. LC-MS/MS analyses of the intact proteins were done as described¹³ with minor modifications. Proteins (2 pmol) were loaded on a C18 pepMap300 guard column (0.3 mm i.d. × 5 mm long, 5 μm particle size, 300 Å pore size, Dionex S. A.) in 40% solvent B (solvent B is 2% (v/v) water/acetonitrile, 0.1% (v/v) formic acid and solvent A is 2% (v/v) acetonitrile/water, 0.05% (v/v) TFA for loading, and 0.1% (v/v) formic acid for elution). Elution from the LC Packing PepMap300 column (75 μm i.d. × 150 mm long, packed with 5 μm particle size, 300 Å pore size, Dionex S. A.) was performed by using a 17 min-linear gradient from 40% to 100% (v/v) of solvent B at 300 nL/min. The time-of-flight mass spectrometry (TOF-MS) survey scan was acquired for 1 s over a mass range of 800–2000 m/z to cover the multiple charge states of the intact proteins and 2 s for MS/MS range of 50–1000 m/z . An information-dependent acquisition method was used with maximum collision energy set to 50 V and with include ion list corresponding to the 13+, 14+, 15+, and 16+ charge states of prolyl-AnaD or its analogues. For these highly charged states, a collision energy of 50 V was critical for the detection of the pantetheine signature fragment ion at mass m/z 261.13 and the dephosphorylated phosphopantetheinyl arm with proline (m/z 358.19) or dehydroproline (m/z 356.17) or analogues attached to it. As already noted, intact prolyl-AnaD and analogues showed minor covalent adducts at $M + 178$ (gluconoylation) and at $M + 97$ (proline linked to the N-terminal amine).^{13,33}

RESULTS

Construction, Production, and Purification of E244A AnaB. We reported that AnaB, which catalyzes the oxidation of prolyl-AnaD in the biosynthesis of anatoxin-a, is a member of the ACAD family of enzymes, as evidenced by protein sequence alignments,¹³ and that it is homologous to hIVD, an enzyme involved in the degradation of fatty acids in humans, for which a three-dimensional structure is available.³⁴ We could thus identify the putative active site base of AnaB, a glutamyl residue, E244, which perfectly aligned with the known active site base of hIVD, E254 (Figure S1). We have now constructed a mutant, E244A AnaB, to study the role of this residue in AnaB-catalyzed reactions. The mutant was constructed using a PCR-based site-directed mutagenesis methodology, and the

sequence of the mutated gene was verified. The recombinant E244A AnaB was purified to homogeneity as judged by separation on gel electrophoresis (Figure S2), and we verified by ESI-MS the integrity of the mutated protein (calculated 46 359.07 Da for the protein lacking the first Met, found 46 359.4 Da). The mutant protein behaved as the wild-type enzyme during chromatographic separation and showed a characteristic electronic absorption spectrum for FAD-containing proteins (Figure 1).

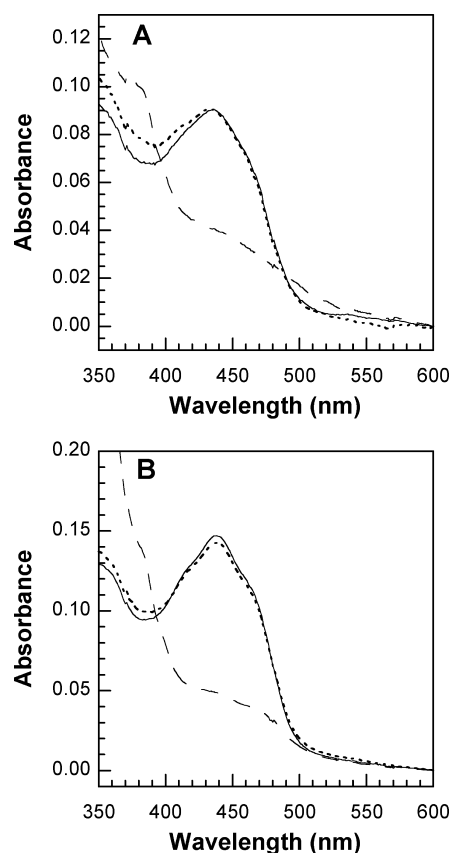


Figure 1. Reduction by dithionite and reoxidation by air of wild-type and E244A AnaB. (A) Electronic absorption spectrum of 7.9 μM recombinant wild-type AnaB before reduction by dithionite (solid line), after reduction by 0.52 mM dithionite (dashed line), and after reoxidation by air (dotted line). (B) Electronic absorption spectrum of 12.8 μM recombinant E244A AnaB before reduction by dithionite (solid line), after reduction by 0.52 mM dithionite (dashed line), and after reoxidation by air (dotted line). The spectra were recorded at room temperature in 20 mM Tris-HCl buffer, pH 7.7, containing 10% v/v glycerol.

Dithionite-Reduced Wild-Type and Mutant AnaB Are Reoxidized by Air. Figure 1A shows the electronic absorption spectrum of recombinant wild-type AnaB in the visible region before addition of dithionite (solid line). This absorption spectrum, in the 350–600 nm range, is characteristic of FAD-containing enzymes. We used excess dithionite (0.52 mM) to reduce the wild-type enzyme (7.9 μM), in a sealed cuvette, and we obtained a characteristic bleaching of the visible spectrum (dashed line). We observed a complete and immediate reoxidation of the enzyme by simply opening the sealed cuvette to air and by inverting the cuvette twice. The spectrum of the reoxidized enzyme (dotted line) was identical

to that of the native enzyme. Thus, AnaB is a flavoprotein that probably uses oxygen as the second substrate, and this enzyme is likely an oxidase rather than a dehydrogenase. We observed the same reduction/reoxidation behavior with E244A AnaB, confirming the integrity of this mutant enzyme (Figure 1B).

Identification of the AnaB-Oxidized Product by HPLC and LC-MS/MS. In our previous study we reported that AnaB catalyzed the two-electron oxidation of prolyl-AnaD, but we were unable to directly observe, by HPLC, the oxidation product because prolyl-AnaD and its oxidation product are unstable due to rapid hydrolysis of their thioester bond, yielding to holo-AnaD.¹³ To facilitate the observation of the oxidized product, we have now optimized the preparation of prolyl-AnaD and its oxidation by using short incubation times and high concentrations of AnaB. Prolyl-AnaD was thus prepared and immediately incubated, without further purification, in the presence of recombinant wild-type AnaB: 60 μ M prolyl-AnaD was oxidized in the presence of 10 μ M AnaB for 5 min. Because we showed that AnaB did not oxidize free proline and that AnaC did not accept free P5C or pyrrole-2-carboxylate as substrates,¹³ any oxidation reaction observed must occur on proline tethered to AnaD. The reaction was analyzed by HPLC, from 0.5 to 7.5 min incubation times (Figure 2A). A new peak at 18.9 min was clearly visible on the HPLC chromatogram, and its intensity increased with incubation time. At longer incubation times, over 7 min, holo-AnaD appeared as a shoulder of the new peak at 18.9 min and became the major product after 10 min incubation time. Although quantification of the product was not very accurate due to overlapping of the peaks, the relative concentration of the product over that of the substrate increased linearly against time, up to 5 min and 50% transformation (Figure 2B). From these data an apparent rate and an apparent catalytic constant could be estimated: $V_{app} = 11 \mu\text{M}/\text{min}$ and $k_{cat,app} = 1 \text{ min}^{-1}$. Thus, AnaB catalyzed the reaction with multiple turnovers and uses oxygen as the second substrate, as suggested above. We did not detect the formation of any new peak in control experiments without AnaB or in the presence of E244A AnaB, as shown in Figure 2A and Figure 2C, respectively. Thus, the E244A AnaB mutant was inactive, as expected.

We then unambiguously identified, by LC-MS/MS, the two species detected by classical HPLC. Figure 3A shows the LC-MS chromatogram, as the total ion current, of the oxidation reaction after 5 min incubation time in the presence of 10 μ M wild-type AnaB, revealing two overlapping peaks. Analysis of the ESI-MS spectra at 15.7 and 16.1 min (Figure S31) gave the following mass: 14 246.6 and 14 244.8 Da, respectively, which corresponded to the calculated average mass for prolyl-AnaD (14 247.2 Da) and dehydropoly-AnaD (14 245.2 Da). The MS/MS spectrum of the 16+ charge states at 15.7 and 16.1 min elution times are shown in Figures 3B and 3C, respectively. In these MS/MS spectra, the ion corresponding to the dephosphorylated phosphopantetheine arm acylated with proline, m/z 358.18 (Figure 3B), or dehydropyrolone, m/z 356.17 (Figure 3C), are clearly visible. This facile fragmentation allowing direct identification of the phosphopantetheine arm, acylated or not, has been coined the “Ppant ejection assay” by its inventors.^{35–37} Moreover, the typical m/z 261.13 ion, which is formed after loss of the acyl moiety of the thioester of the dephosphorylated arm, is also clearly visible in the MS/MS spectra. We did not observe, as we previously noted,¹³ the putative four-electron oxidation product, pyrrole-2-carboxyl-

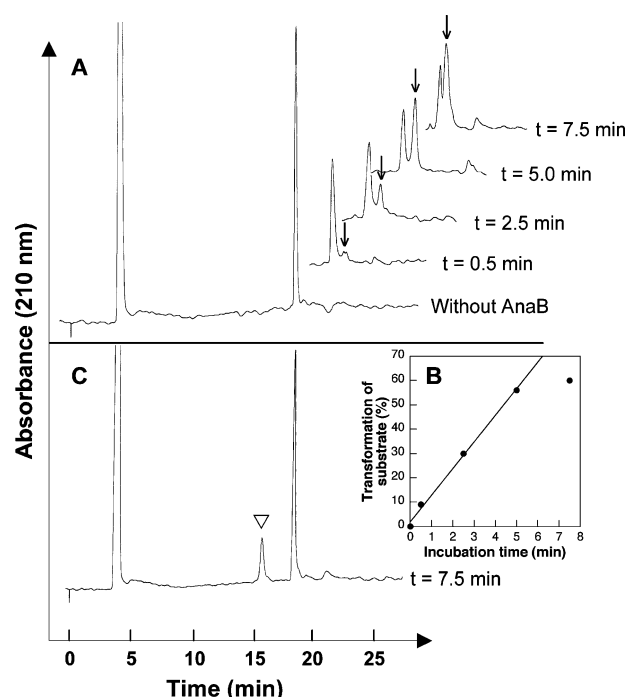


Figure 2. HPLC analysis of the AnaB-catalyzed oxidation of prolyl-AnaD. A solution of prolyl-AnaD (60 μ M) was incubated in the absence or in the presence of 10 μ M AnaB at 28 °C. The reaction was stopped at different time points, and 20 μ L aliquots were analyzed by HPLC. (A) From bottom to top: chromatogram of the reaction in the absence of AnaB, and portion of the chromatograms of the reactions run in the presence of 10 μ M wild-type recombinant AnaB at 0.5, 2.5, 5.0, and 7.5 min incubation time. The oxidation product is marked by an arrow. AnaB eluted at 15.5 min but is not shown here for clarity. The absorption in the void volume (4 min) is mainly due to the ATP used in the loading of proline on holo-AnaD. (B) The relative amount of product was plotted against incubation time. The first data points were fitted to a straight line (slope = 11% per min, $r = 0.99$). (C) A control experiment was run in the presence of 10 μ M E244A recombinant AnaB (7.5 min incubation time, 20 μ L injected). E244A AnaB eluted at 15.5 min (marked with a triangle).

AnaD, that could be formed after two successive AnaB-catalyzed oxidation reactions. Two control experiments, one without AnaB and the other one in the presence of 10 μ M E244A AnaB, were run (Figures S4 and S5), and in both cases we did not observe any oxidation product, as we observed using classical HPLC (Figure 2).

Synthesis of Deuterium-Labeled Proline and the Corresponding Prolyl-AnaD. In our previous study, we proposed that the oxidation reaction catalyzed by AnaB took place in two steps: first, formation of the conjugated double bond (C2=N) with hydride transfer to the flavin and, then, an aza-allylic isomerization to form the C5=N double bond.¹³ Indeed, the proposed AnaB product, in the biosynthesis of anatoxin-a and homoanatoxin-a, is P5C-AnaD.^{9,13} To challenge this proposition, we have now prepared three deuterium-labeled analogues of proline as depicted in Scheme 2. The reaction sequences are based on published procedures or are adaptation of these procedures.^{29–32} Labeling at position C2 was achieved by racemization of proline in the presence of PLP in D_2O .^{29,30} We obtained *rac*-[2- 2H]-proline **1**, containing 97% deuterium, as determined by 1H NMR, only after three rounds of this step. The doubly labeled [5,5- 2H_2]-L-proline **5** was

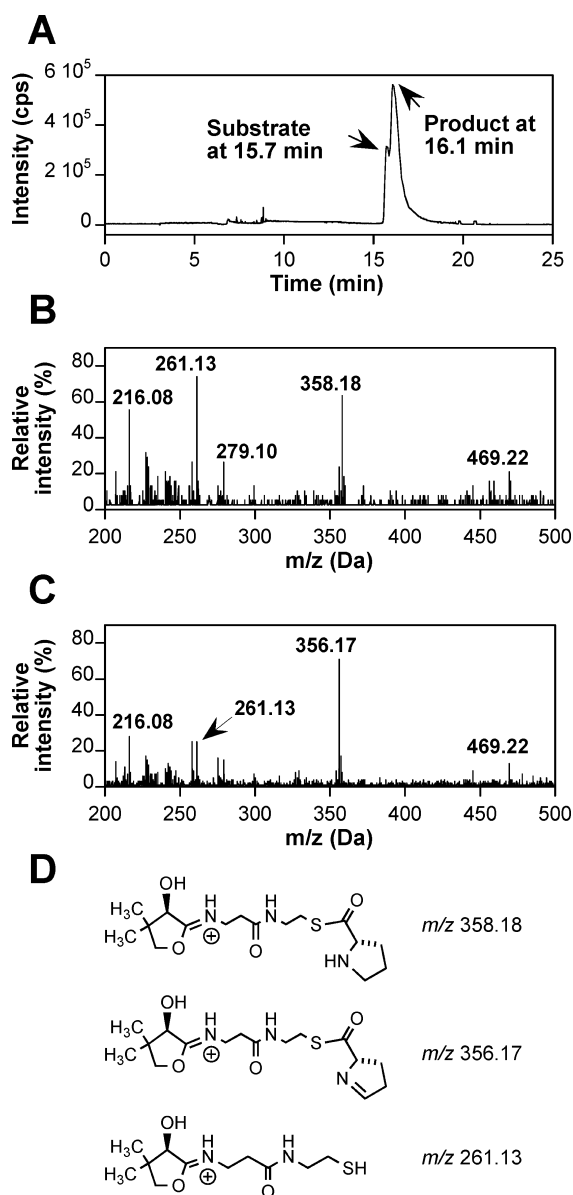
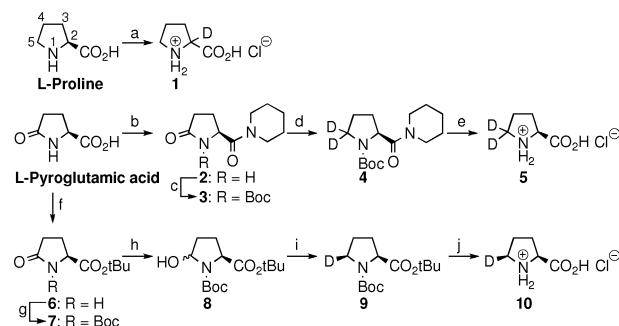


Figure 3. LC-MS/MS analysis of the AnaB-catalyzed oxidation of prolyl-AnaD. The oxidation reaction mixture containing 60 μ M prolyl-AnaD and 10 μ M wild-type AnaB and incubated at 28 $^{\circ}$ C for 5 min was analyzed by LC-MS/MS. (A) The total ion current chromatogram is shown. AnaB was not observed under these separation conditions because it was not retained on the precolumn. (B) MS/MS spectrum at 15.79 min of the 16+ charge state of the substrate. (C) MS/MS spectrum at 16.11 min of the 16+ charge state of the product. (D) Structure and calculated mass for the detected ions.

obtained using an interesting regioselective reduction of Boc-L-pyrroglutamic piperidine amide **3** by NaBD₄ in the presence of iodine. This reaction has been applied to diverse amides and lactams,³¹ but we have used it for the first time on Boc-pyrroglutamic amide. The overall deuterium content of compound **5** was 91% with an equal labeling of both C5 positions, as determined by ¹H NMR. We used a stereoselective reduction of hemiaminal **8**, the *tert*-butyl ester of Boc-L-glutamate semialdehyde, by Bu₃SnD containing 96% deuterium, to specifically labeled the C5-*pro*-S position of proline.³² However, the reduction was not fully stereoselective and gave 85% labeling at the C5-*pro*-S position and 15% at the

Scheme 2. Outline of the Synthesis of Deuterium Labeled Prolines^a



^aKeys: a: NaOD, PLP, D₂O, purification on ion-exchange resin. This process was repeated three times. b: HOBT, DCC, piperidine, THF. c: DMAP, Boc₂O, CH₃CN. d: NaBD₄, I₂, THF. e: TFA, CH₂Cl₂, then neutralization with NaOH and purification on ion-exchange resin. f: *tert*-Butyl acetate, HClO₄. g: DMAP, Boc₂O, THF. h: DIBAL-H, THF. i: Bu₃SnD, toluene. j: TFA, CH₂Cl₂, then 2 M HCl.

C5-*pro*-R position, as determined by careful examination of the ¹H NMR spectrum of compound **10**. Thus, compound **10** is a mixture of 82% of (5R)-[5-²H]-L-proline and 14% of (5S)-[5-²H]-L-proline and 4% of unlabeled proline. We also used the perdeuterated proline, [2,3,3,4,4,5,5-²H₇]-L-proline, containing 97–98% deuterium, obtained from commercial source. All deuterated prolines were substrate of AnaC, the adenylation protein that transforms holo-AnaD into prolyl-AnaD,^{9,13} and we verified by HPLC that the reactions were all complete. Because we showed in our previous report that D-proline is not a substrate for AnaC,¹³ we obtained [2-²H]-L-prolyl-AnaD using compound **1**, which is a racemate. All these deuterium-labeled prolyl-AnaD were then directly used in the AnaB-catalyzed oxidation reaction, as described above for unlabeled prolyl-AnaD.

LC-MS/MS Analysis of the AnaB-Catalyzed Oxidation Reaction Using Deuterium-Labeled Prolyl-AnaDs. The oxidation reactions, and control experiments either in the absence of AnaB or in the presence of E244A AnaB, were analyzed by LC-MS/MS. We could measure the mass of the substrates and of the products (Table 1) and also detect, in the MS/MS spectra, the pantetheine thioester ion ejected from the substrates or from the products and analyze its isotopic distribution (Table 2 and Figure S17). The substrates were all labeled according to the deuterium labeling of the proline used to prepare them, and the observed isotopic distributions of the acylated pantetheine ion matched that of calculated ones (Figure S17).

We observed a partial loss (~50%) of the deuterium labeling on position C2 of the remaining substrate, at ~50% transformation, in the presence of wild-type AnaB (Table 2, entry 4). This deuterium loss was absent in the untreated substrate (Table 2, entry 2) and in the substrate that was treated with the E244A mutant (Table 2, entry 3). Furthermore, we also observed this partial loss, at the substrate level, when we used [2H₇]-L-prolyl-AnaD (Table 2, entries 7–9). Indeed, in the absence of AnaB or in the presence of E244A AnaB (Table 2, entries 7 and 8), we observed the expected ion *m/z* 365.22 and the ion *m/z* 364.22, as a minor species, arising from all species containing six deuteriums (Figure S17). This isotopic distribution was reversed in the remaining substrate when treated with wild-type AnaB (Table 2, entry 9). This loss

Table 1. Summary of the Calculated and Observed Mass for the Different AnaD Forms Characterized in This Report

protein	calcd av mass (Da) ^a	obsd av mass (Da)	Figure in Supporting Information
holo-AnaD	14 150.12	14 150.2 ^b	
prolyl-AnaD	14 247.28	14 246.6 ^c	S3
dehydroprolyl-AnaD	14 245.22	14 244.8 ^c	S3
[2- ² H]-L-prolyl-AnaD	14 248.25	14 247.2 ^c	S6, S7, S8
[5,5- ² H ₂]-L-prolyl-AnaD	14 249.25	14 248.3 ^c	S9
(5S)-[5- ² H]-L-prolyl-AnaD	14 248.25	14 247.1 ^c	S10
[5- ² H]-dehydroprolyl-AnaD	14 246.23	14 245.4 ^c	S9, S10
[2,3,3,4,4,5,5- ² H ₇]-L-prolyl-AnaD	14 254.28	14 253.5 ^c	S11, S12
[² H ₅]-dehydroprolyl-AnaD	14 250.25	14 250.0 ^{c,d}	S13
3,4-dehydro-L-prolyl-AnaD	14 245.22	14 244.7 ^c	S14
(4S)-4-fluoro-L-prolyl-AnaD	14 265.23	14 264.4 ^c	S15
(4R)-4-fluoro-L-prolyl-AnaD	14 265.23	14 264.6 ^c	S16
pyrrole-2-carboxyl-AnaD	14 243.21	14 242.7 ^c	S14–S16

^aThe calculated masses correspond to the recombinant protein lacking the N-terminal Met1. ^bTaken from our previous reports.^{9,13} ^cA minor species corresponding to the formation of an amide, probably on the N-terminal amine, with the proline or proline analogue used during the AnaC-catalyzed loading on holo-AnaD, was also observed. The minor gluconoylated M+178 species was always present.³³ ^dThis sample is in fact a mixture of several isotopologues.

of labeling at position C2 is likely due to a rapid enolization catalyzed by AnaB, as discussed below. The experiment using [²H₇]-L-prolyl-AnaD and the inactive E244A AnaB mutant (Table 2, entry 8) showed that no deuterium loss was observed on any position of the substrate, thus serving as a control experiment for all other experiments described in Table 2.

We clearly observed a complete loss of deuterium in the MS/MS spectrum of the product obtained after AnaB-catalyzed oxidation of [2-²H]-L-prolyl-AnaD (Table 2, entry 4). The isotopic distribution of the ion ejected from the product corresponded to an unlabeled ion (*m/z* 356.17, Figure S17). When the substrate, either doubly labeled on position C5 or labeled on position C5-*pro-S*, was oxidized, we observed a major ion at *m/z* 357.18 (Table 2, entries 5 and 6; see Scheme 3 for identification of the prochiral hydrogens of proline). This is consistent with a stereospecific retention of deuterium on position C5-*pro-S* after oxidation and a loss of the deuterium on position C5-*pro-R*, as discussed below. The isotopic distribution of the ion detected in the MS/MS spectrum of the product when using [²H₇]-L-prolyl-AnaD was more complex than expected (Table 2, entry 9). The *m/z* 358.18, 359.21, and 360.20 ions were observed in approximate equal intensity together with the *m/z* 356.15, 357.19, and 361.18 ions as minor species. These data revealed incomplete exchanges on other positions than the C2 and C5-*pro-R* positions, as discussed below. The data presented in Table 2 were confirmed using an alternate strategy that we previously described,¹³ consisting in a trypsin digestion of the substrate and product of AnaB-catalyzed reactions, followed by LC-MS/MS analysis of the

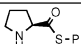
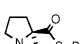
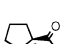
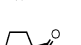
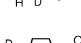
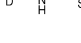
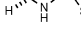

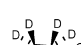
digest. However, we considered the data presented in Table 2 more reliable because nonspecific deuterium exchanges could occur during the trypsin digestions.

LC-MS/MS Analysis of the AnaB-Catalyzed Oxidation Reaction Using Analogues of Prolyl-AnaD. In our previous report we showed that AnaC, the adenylation protein, was very specific for L-proline but that it accepted some close structural analogues of proline as substrates.¹³ We took advantage of this narrow substrate promiscuity to load onto holo-AnaD, 3,4-dehydro-L-proline and the two diastereoisomers of 4-fluoro-L-proline. We obtained the three corresponding prolyl-AnaD analogues, that were characterized by HPLC and LC-MS/MS (Tables 1 and 3). These prolyl-AnaD analogues were used in typical AnaB-catalyzed oxidation reactions and analyzed as described for prolyl-AnaD (Table 3). When 3,4-dehydro-L-prolyl-AnaD was oxidized by AnaB we observed on the LC-MS chromatogram (Figure S14) a large transformation of the substrate, suggesting that 3,4-dehydro-L-prolyl-AnaD is a very good substrate for AnaB. As expected, we observed, on the MS/MS spectrum of the product, the *m/z* 354.16 ion, which is most likely the daughter ion arising from pyrrole-2-carboxyl-AnaD (Table 3, entry 1). (4S)- and (4R)-4-fluoro-L-prolyl-AnaD, neatly detected by LC-MS/MS (*m/z* 376.18), were substrates of AnaB and gave, as the only detectable product, pyrrole-2-carboxyl-AnaD (*m/z* 354.16, Table 3, entries 2 and 3). However, the (4S)-4-fluoro-L-prolyl-AnaD (*cis*-isomer) was a poor substrate compared to the *trans*-isomer (Figures S15 and S16). Thus, both diastereoisomers were oxidized by AnaB and experienced rapid elimination of HF because we could not detect the intermediate, 4-fluoro-dehydroprolyl-AnaD. This elimination is most likely explained by formation of a conjugated carbanion on position C5, during the AnaB-catalyzed aza-allylic isomerization, as discussed below. The E244A AnaB mutant was inactive toward these fluoro- or dehydroprolyl-AnaD substrates, as determined in control experiments analyzed by HPLC.

DISCUSSION

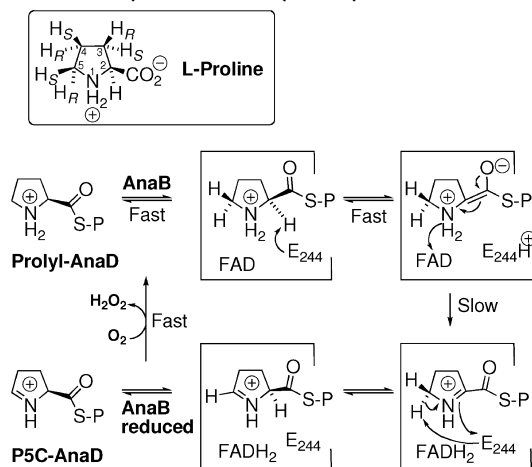
On the basis of sequence alignments, we showed that AnaB belongs to the ACAD superfamily.¹³ Using more specific alignments, we showed that AnaB and the prolyl-ACP dehydrogenases that are involved in the pyrrole ring formation of secondary metabolites, such as pyoluteorin,^{14,19} prodigine,¹⁶ clorobiocin,^{17,20} prodigiosin,^{18,21} or leupyrrin,²⁶ for instance, have all a strictly conserved glutamyl residue that corresponds to the hIVD active site base (E254). In contrast, the active site base of the pig medium chain acyl-CoA dehydrogenase (MCAD), E376, is not conserved in AnaB. We have mutated the conserved glutamyl residue in AnaB into an alanyl residue and showed that this E244A AnaB mutant contains a FAD cofactor and that it retains the flavin redox properties but is completely inactive toward prolyl-AnaD. Hence, this residue is probably the AnaB active site base. However, after reduction by dithionite, AnaB is completely and very rapidly reoxidized by molecular oxygen. This is in sharp contrast to the very slow reactivity of ACAD with molecular oxygen.^{38,39} Thus, AnaB, and probably the other prolyl-ACP dehydrogenases, are oxidases rather than dehydrogenases. The structural basis for this different reactivity toward oxygen must await the solution of the three-dimensional structure of AnaB. Thus, AnaB and hIVD share sequence identity and strong

Table 2. Summary of the LC-MS/MS Analysis of the AnaB-Catalyzed Oxidation Reaction Using the Deuterium-Labeled Prolyl-AnaD as Substrates^a

entry	substrate ^a	deuterium labeling (%)	enzyme used	MS/MS analysis (ion detected and approximate relative intensity) ^b		Figure in Supporting Information
				substrate (<i>m/z</i>)	product (<i>m/z</i>)	
1		0	WT AnaB	358.19	356.17	S3
2		97	no enzyme	359.19	ND ^c	S6
3		97	E244A AnaB	359.19	ND	S7
4		97	WT AnaB ^d	358.19 (iso) 359.19 (iso)	356.17	S8
5		91	WT AnaB	360.20 (maj) 359.19 (min)	357.18 (maj) 356.17 (min)	S9
6		85	WT AnaB	359.19 (maj) 358.19 (min)	357.18 (maj) 356.17 (min)	S10
7		97-98 ^e	no enzyme	365.22 (maj) 364.22 (min) ^f	ND	S11
8		97-98	E244A AnaB	365.22 (maj) 364.22 (min)	ND	S12
9		97-98	WT AnaB	365.23 (min) 364.22 (maj)	361.18 (min) 360.20 (iso) 359.21 (iso) 358.18 (iso) 357.19 (min) 356.15 (min)	S13

^aFootnotes: *a*: P represents the holo-AnaD protein. *b*: The isotopic distributions of the detected ions are shown in Figure S17 and were compared to simulated distributions. The relative intensities are only given here as a qualitative estimate: maj: major ion detected; min: minor ion detected; iso: ions of approximate equal abundance. *c*: ND: not detected. *d*: In this experiment we used 5 μ M wild-type AnaB rather than 10 μ M to reduce the substrate transformation for an easier LC-MS/MS analysis of the remaining substrate. *e*: As indicated by the manufacturer. *f*: This ion arose from the molecules containing six deuterium rather than seven. See Figure S17 for further interpretation of the isotopic distributions.

Scheme 3. Proposed Reaction Mechanism for the Oxidation Reaction of Prolyl-AnaD Catalyzed by AnaB^a



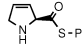
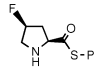
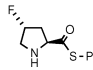
^aP represents the holo-AnaD protein.

mechanistic similarities, as discussed below, but differ in their reactivity toward molecular oxygen.

By using controlled incubation conditions, we have been able to observe, by HPLC and LC-MS/MS, the AnaB product, dehydroproyl-AnaD. We could also observe multiple turnovers by AnaB, but unfortunately, due to intrinsic instability of the substrate and low sensitivity of the detection of the product by HPLC coupled to a UV detector, we have not yet been able to conduct thorough kinetic analysis of the AnaB-catalyzed reaction but estimated an apparent catalytic constant of 1 min⁻¹. This value is much lower than that reported for MCAD,³⁸ for instance, and it is not clear at the moment why AnaB catalysis is so slow. It might be possible that AnaB efficiency depends on some specific protein–protein interactions with the PKS AnaE, to which AnaB product is thought to be transferred.

To study in detail the reaction mechanism of AnaB, we have prepared several deuterium-labeled prolines and their corresponding prolyl-AnaD proteins. These proteins were substrates of AnaB, and we could analyze by LC-MS/MS, thanks to the so-called “Ppant ejection assay”,^{35–37} the fate of the deuterium

Table 3. Summary of the LC-MS/MS Analysis of the AnaB-Catalyzed Oxidation Reaction Using 3,4-Dehydro-L-Prolyl-AnaD and *cis*- and *trans*-4-Fluoro-L-Prolyl-AnaD^a

entry	substrate ^a	enzyme used	MS/MS analysis		Figure Supporting Information
			substrate (<i>m/z</i>)	product (<i>m/z</i>)	
1		WT AnaB	356.17	354.16	S14
2		WT AnaB	376.18	354.16	S15
3		WT AnaB	376.18	354.16	S16

^aP represents the holo-AnaD protein.

labeling in the substrates and products. First, we conclusively observed a partial loss of the C2-D deuterium, and hence the C2–H proton in the unlabeled substrate, on prolyl-AnaD in the presence of wild-type AnaB. This is most consistent by assuming that AnaB catalyzes a fast enolization, as depicted in Scheme 3, and that its protonated active site base (E244) exchanges rapidly its proton with the solvent. Observation of this exchange suggests that all physical and chemical steps prior to hydride transfer to the FAD cofactor are faster than the redox chemical step. This, again, is in contrast to the situation in ACAD, which do not show, during turnover of good substrates, such exchange on the C2–H proton of the acyl-CoA substrate.³⁸

Second, we observed, in the two electron-oxidized product, a complete loss of the labeling at positions C2, as revealed by the isotopic distribution of the ejected ion of the product (Figure S17). This is consistent with the formation of the P2C-AnaD imine as depicted in Scheme 3. Third, we observed a loss of labeling at position C5 that could, in principle, be explained by either an exchange of the C5-deuterium with solvent proton on the P2C-AnaD imine or a loss of deuterium during the P2C-AnaD to P5C-AnaD isomerization. By using a doubly labeled substrate on C5 with symmetrical labeling on that position and a singly labeled substrate, which is mainly labeled on the C5-*pro-S* position, we could discriminate among these possibilities. Figure 4 shows the predicted isotopic distribution of the ion ejected from the product, for all these possibilities, together with the experimental isotopic patterns obtained using both substrates. Clearly, the experimental data fitted very well to the prediction for a stereospecific loss of the C5-*pro-R* deuterium. However, these experiments cannot discriminate between a stereospecific loss of the C5-*pro-R* deuterium to form P5C-AnaD and a complete stereospecific exchange of the same deuterium on P2C-AnaD. In other words, we cannot at the moment obtain any information on the position of the equilibrium between P2C-AnaD and P5C-AnaD. Attempts to quench the product with specific reagents (NaBD₄, 2-aminobenzaldehyde, or 2,4-dinitrophenylhydrazine) for further spectroscopic analysis have so far been unsuccessful.

The fact that the loss of deuterium at position C5 is stereospecific strongly suggests that we are observing an enzyme-catalyzed reaction rather than a nonspecific exchange occurring in solution after release of the product. These data

are consistent with the proposed AnaB reaction mechanism involving formation of an imine at position C2=N in the first step, followed by an aza-allylic isomerization in the second step (Scheme 3). This isomerization is very likely catalyzed by the same active site base, E244, because the two deuterons or protons that are lost or exchanged are on the same side of the 5-membered cycle of the substrate, intermediate or product (the *Re-Re* prochiral face of the imines). There are precedents for this catalyzed isomerization in ACAD and homologous enzymes. Indeed, this isomerase activity has been observed in MCAD on various substrates or inhibitors.^{40–42} Furthermore, Liu and colleagues suggested that this isomerization, observed in ACAD, was catalyzed by one base, the actual glutamyl active site base.^{40,41} Interestingly, in the biosynthesis of the antibiotic friulimycin in *Actinoplanes friuliensis*, a flavoprotein, LipB, homologous to ACAD, has been identified, and it was shown that it catalyzed the formation of the Δ*cis*3 double bond (C3=C4 *Z*-double bond) of the acyl-ACP starter.^{43,44} Thus, in this ACAD, the aza-allylic isomerization is fully operative and yields to the unconjugated less stable product.

The abstraction of the C5–H-*pro-R* was also substantiated by observation of the HF elimination when *cis*- or *trans*-4-fluoro-L-prolyl-AnaD was used as a substrate. The *cis*-isomer was a much poorer substrate than the *trans*-isomer, but both gave, as unique product, the pyrrole-2-carboxyl-AnaD. This is consistent with the formation of a conjugated carbanion on position C5 followed by a rapid elimination of fluorine (Scheme 4). This elimination is thus of the E1cB type although the relative rates of both steps (proton abstraction and elimination) cannot at this point be determined.

We also observed some exchange of deuterium at other positions than C2 and C5-*pro-R*, in the AnaB-catalyzed oxidation of the perdeuterated [²H₇]-L-prolyl-AnaD, because the isotopic distribution of the ejected ion showed the presence of ions from *m/z* 356 to *m/z* 361 (Figure S17). Because the deuterium on position C5-*pro-S* is retained, there are four positions left for possible exchanges that are positions at C3 and C4. This is chemically sound because these exchanges could occur during enamine–imine tautomerisms. We have calculated the isotopic distribution of the ion ejected from the product if these four different positions would independently exchange 50% of their deuterium (at the same rate) with the solvent protons (Figure S17). This oversimplified calculation

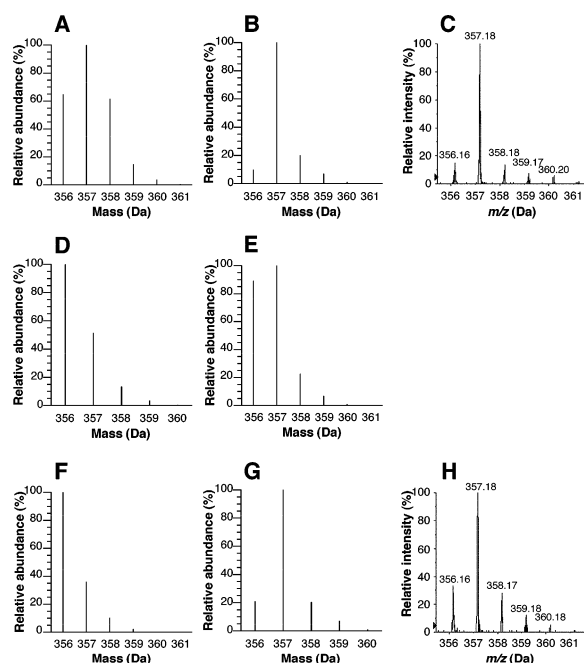
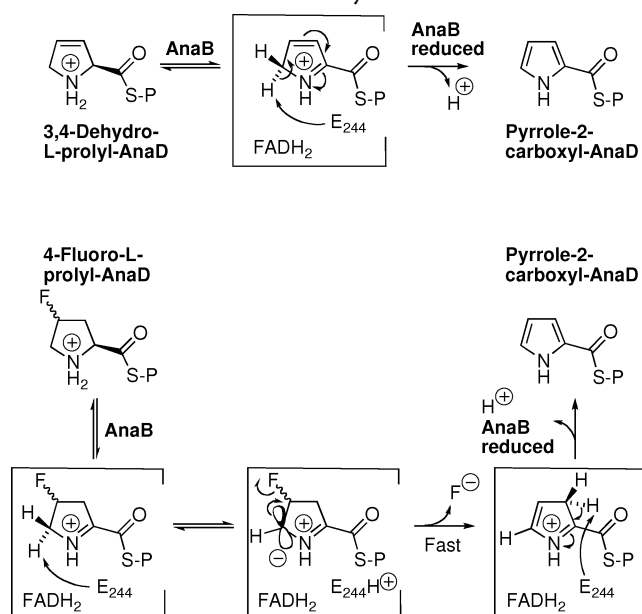


Figure 4. Simulated and experimental isotopic distributions of the acylated pantetheine ion ejected from the product after AnaB-catalyzed oxidation of [S,S-²H₂]-L-prolyl-AnaD (A–C) and (S,S)-[S-²H₁]-L-prolyl-AnaD (D–H). (A) Simulated isotopic distribution of the ion from the oxidized product of [S,S-²H₂]-L-prolyl-AnaD, assuming a nonstereoselective partial exchange (50% on each position and independently) of deuterium with proton at position C5 of the P2C-AnaD imine. (B) Simulated isotopic distribution of the ion from the oxidized product of [S,S-²H₂]-L-prolyl-AnaD, assuming a stereoselective loss (at C5-*pro-R* or C5-*pro-S*) or nonstereoselective loss of deuterium at position C5, to form P5C-AnaD. The same pattern is obtained for these three possibilities because the labeling is symmetrical in this substrate. (C) Experimental isotopic distribution of the ion from the AnaB oxidized product of [S,S-²H₂]-L-prolyl-AnaD. (D) Simulated isotopic distribution of the ion from the oxidized product of (S,S)-[S-²H₁]-L-prolyl-AnaD, assuming a nonstereoselective exchange (50% on each position and independently) of deuterium with proton at position C5 of the P2C-AnaD imine. (E) Simulated isotopic distribution of the ion from the oxidized product of (S,S)-[S-²H₁]-L-prolyl-AnaD, assuming a nonstereoselective loss of deuterium at position C5, to form P5C-AnaD. (F) Simulated isotopic distribution of the ion from the oxidized product of (S,S)-[S-²H₁]-L-prolyl-AnaD, assuming a stereoselective loss of deuterium at position C5-*pro-S*, to form P5C-AnaD. (G) Simulated isotopic distribution of the ion from the oxidized product of (S,S)-[S-²H₁]-L-prolyl-AnaD, assuming a stereoselective loss of deuterium at position C5-*pro-R*, to form P5C-AnaD. (H) Experimental isotopic distribution of the ion from the AnaB oxidized product of (S,S)-[S-²H₁]-L-prolyl-AnaD. The methods used to simulate the isotopic distributions are described in Figure S17.

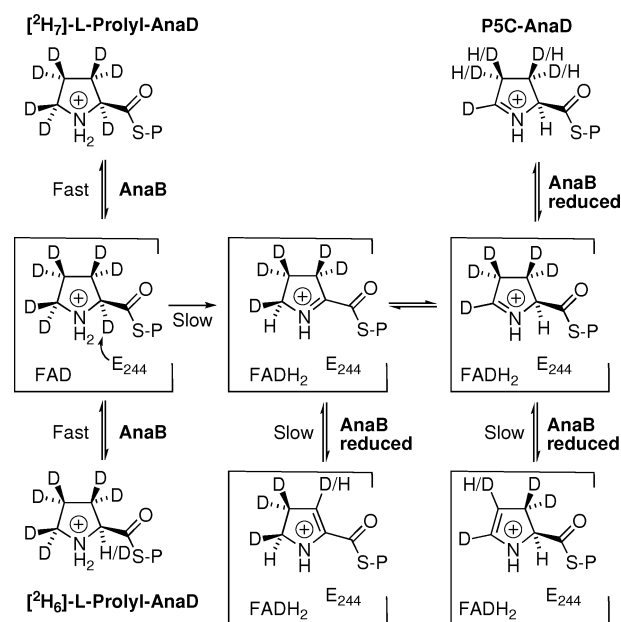
shows that the major species observed will be the D₂, D₃, and D₄ species (at 65%, 100%, and 75% normalized relative intensities). We observed ions at *m/z* 358, 359, and 360 with approximately the same abundance in the MS/MS spectrum of the ion ejected from the oxidation product of [²H₇]-L-prolyl-AnaD (Table 2 and Figure S17). Thus, it is reasonable to propose that the C3 and C4 positions, in the P5C-AnaD and P2C-AnaD imines could experience exchanges via the enamine–imine tautomerism (Scheme 5). However, these exchanges have to be nonstereospecific to explain the loss of deuterium on four different positions. Thus, the E244 base

Scheme 4. Proposed Reaction Mechanism for AnaB-Catalyzed Half-Reaction with 3,4-Dehydro-L-Prolyl-AnaD and *cis*- or *trans*-4-Fluoro-L-Prolyl-AnaD^a



^aP represents the holo-AnaD protein.

Scheme 5. Proposed Mechanism for the Observed Exchange of Deuterium at Positions C3 and C4 of [²H₇]-L-Prolyl-AnaD^a



^aP represents the holo-AnaD protein.

could abstract all deuterium/proton on the lower face of the molecule, but the reprotonation on position C3 and C4 should be nonstereospecific. Perhaps a water molecule present in the active site or another base could catalyze these reprotonations on the upper face. There are indeed water molecules present in the active site of ACAD, although binding of the acyl-CoA substrate expels some of them.³⁸ We cannot exclude that the observed exchanges could occur in solution after the product is released from the active site of AnaB, but several studies have

shown that the isomerization of P5C into P2C and the enamine–imine equilibrium in these imines are very slow at pH 7.^{45–47} We thus believe that all exchanges observed in this report are catalyzed by AnaB and that the loss of deuterium/proton on positions C2 and C5-*pro-R* must be in the reaction path since they are complete while the other exchanges are not part of the reaction path since they are not complete.

The fact that 3,4-dehydro-L-prolyl-AnaD is a very good substrate for AnaB and that it gave pyrrole-2-carboxyl-AnaD excludes this molecule as a possible intermediate in the reaction path of AnaB. Walsh and co-workers had already observed that the prolyl-ACP dehydrogenase, CloN3, also transformed 3,4-dehydro-L-prolyl-ACP into pyrrole-2-carboxyl-ACP.^{20–22} They interpreted that result by invoking that 3,4-dehydroprolyl-ACP could be an intermediate in the reaction path of this four-electron oxidation reaction, and this would be the mechanistic difference between AnaB and CloN3. However, it could also be possible that CloN3 utilizes the same reaction path than AnaB but displaces the isomerizations toward the C4=C5 enamine that would be then oxidized in a second round to yield the pyrrole aromatic ring. The difference between AnaB and CloN3 reaction paths would then be the concentration and lifetime in the active site of the C4=C5 enamine: low concentration and short lifetime in AnaB versus high concentration and long lifetime in CloN3. This interesting issue might only be solved when we will have in hand the three-dimensional structure of these enzymes to compare their active site structures and detailed kinetic studies on these enzymes.

In conclusion, we report here evidence that support the proposed reaction mechanism for AnaB, involving the rapid formation of an enolate followed by hydride transfer to the flavin, to form the P2C-AnaD imine, which in turn is isomerized to P5C-AnaD, the product. We have identified the active site base, glutamyl residue E244, which probably serves as a base during enolization and isomerization.

■ ASSOCIATED CONTENT

● Supporting Information

Figure S1: sequence alignments of AnaB and hIVD; Figure S2: gel electrophoresis of AnaB proteins; Figures S3–S16: LC-MS/MS analysis of the oxidation reactions; Figure S17: analysis of the isotopic distribution of the detected ions for deuterium-labeled molecules. This material is available free of charge via the Internet at <http://pubs.acs.org>.

■ AUTHOR INFORMATION

Corresponding Author

*Tel: +(33) 1 44 27 67 01. E-mail: olivier-ploux@enscp.fr.

Funding

This work was supported by the CNRS and the ENSCP. The Laboratory of Proteomic Mass Spectrometry is supported by grants from “Cancéropôle Ile-de-France” and from the “Institut National du Cancer, INCa”.

■ ACKNOWLEDGMENTS

We thank Santebala Sivacoumarane for technical help during the preparation of prolyl-AnaD and its analogues as well as during the HPLC analysis of the AnaB-catalyzed oxidation reactions.

■ ABBREVIATIONS

ACAD, acyl-CoA dehydrogenase; ACP, acyl carrier protein; Boc, *tert*-butoxycarbonyl; Boc₂O, di-*tert*-butyl dicarbonate; DCC, *N,N*-dicyclohexylcarbodiimide; DIBAL-H, diisobutylaluminum hydride; DMAP, 4-(dimethylamino)pyridine; ESI-MS, electrospray ionization mass spectrometry; hIVD, human isovaleryl-CoA dehydrogenase; HOBt, 1-hydroxybenzotriazole; HPLC, high performance liquid chromatography; IPTG, isopropyl- β -D-thiogalactopyranoside; LB, lysogeny broth; LC-MS/MS, liquid chromatography coupled to tandem mass spectrometry; MCAD, medium chain acyl-CoA dehydrogenase; P2C, 1-pyrroline-2-carboxylic acid; P5C, (S)-1-pyrroline-5-carboxylic acid; PCC, Pasteur culture collection of cyanobacteria; PKS, polyketide synthase; PLP, pyridoxal-5'-phosphate; TCEP, tris(2-carboxyethyl)phosphine; TFA, trifluoroacetic acid; THF, tetrahydrofuran; TOF-MS, time-of-flight mass spectrometry.

■ REFERENCES

- (1) vanApeldoorn, M. E., van Egmond, H. P., Speijers, G. J., and Bakker, G. J. (2007) Toxins of cyanobacteria. *Mol. Nutr. Food Res.* 51, 7–60.
- (2) Edwards, C., Beattie, K., Scrimgeour, C., and Codd, G. (1992) Identification of anatoxin-a in benthic cyanobacteria (blue-green algae) and in associated dog poisoning at Loch Insh, Scotland. *Toxicon* 30, 1165–1175.
- (3) Gugger, M., Lenoir, S., Berger, C., Ledreux, A., Druart, J. C., Humbert, J. F., Guette, C., and Bernard, C. (2005) First report in a river in France of the benthic cyanobacterium *Phormidium favosum* producing anatoxin-a associated with dog neurotoxicosis. *Toxicon* 45, 919–928.
- (4) Cadel-Six, S., Peyraud-Thomas, C., Briant, L., Tandeau de Marsac, N., Rippka, R., and Méjean, A. (2007) Different genotypes of anatoxin-producing cyanobacteria coexist in the Tarn River, France. *Appl. Environ. Microbiol.* 73, 7605–7614.
- (5) Wood, S. A., Selwood, A. I., Rueckert, A., Holland, P. T., Milne, J. R., Smith, K. F., Smits, B., Watts, L. F., and Cary, C. S. (2007) First report of homoanatoxin-a and associated dog neurotoxicosis in New Zealand. *Toxicon* 50, 292–301.
- (6) Puschner, B., Hoff, B., and Tor, E. R. (2008) Diagnosis of anatoxin-a poisoning in dogs from North America. *J. Vet. Diagn. Invest.* 20, 89–92.
- (7) Puschner, B., Pratt, C., and Tor, E. R. (2010) Treatment and diagnosis of a dog with fulminant neurological deterioration due to anatoxin-a intoxication. *J. Vet. Emerg. Crit. Care (San Antonio)* 20, 518–522.
- (8) Wonnacott, S., and Gallagher, T. (2006) The chemistry and pharmacology of anatoxin-a and related homotropans with respect to nicotinic acetylcholine receptors. *Mar. Drugs* 4, 228–254.
- (9) Méjean, A., Mann, S., Maldiney, T., Vassiliadis, G., Lequin, O., and Ploux, O. (2009) Evidence that biosynthesis of the neurotoxic alkaloids anatoxin-a and homoanatoxin-a in the cyanobacterium *Oscillatoria* PCC 6506 occurs on a modular polyketide synthase initiated by L-proline. *J. Am. Chem. Soc.* 131, 7512–7513.
- (10) Cadel-Six, S., Iteman, I., Peyraud-Thomas, C., Mann, S., Ploux, O., and Méjean, A. (2009) Identification of a polyketide synthase coding sequence specific for anatoxin-a-producing *Oscillatoria* cyanobacteria. *Appl. Environ. Microbiol.* 75, 4909–4912.
- (11) Wood, S. A., Heath, M. W., Kuhajek, J., and Ryan, K. G. (2010) Fine-scale spatial variability in anatoxin-a and homoanatoxin-a concentrations in benthic cyanobacterial mats: implication for monitoring and management. *J. Appl. Microbiol.* 109, 2011–2018.

- (12) Ballot, A., Fastner, J., Lentz, M., and Wiedner, C. (2010) First report of anatoxin-a-producing cyanobacterium *Aphanizomenon issatschenkoi* in northeastern Germany. *Toxicon* 56, 964–971.
- (13) Méjean, A., Mann, S., Vassiliadis, G., Lombard, B., Loew, D., and Ploux, O. (2010) In vitro reconstitution of the first steps of anatoxin-a biosynthesis in *Oscillatoria* PCC 6506: from free L-proline to acyl carrier protein bound dehydropyrolidine. *Biochemistry* 49, 103–113.
- (14) Nowak-Thompson, B., Chaney, N., Wing, J. S., Gould, S. J., and Loper, J. E. (1999) Characterization of the pyoluteorin biosynthetic gene cluster of *Pseudomonas fluorescens* Pf-5. *J. Bacteriol.* 181, 2166–2174.
- (15) Wang, Z. X., Li, S. M., and Heide, L. (2000) Identification of the coumermycin A(1) biosynthetic gene cluster of *Streptomyces rishiriensis* DSM 40489. *Antimicrob. Agents Chemother.* 44, 3040–3048.
- (16) Cerdeño, A. M., Bibb, M. J., and Challis, G. L. (2001) Analysis of the prodigiosin biosynthesis gene cluster of *Streptomyces coelicolor* A3(2): new mechanisms for chain initiation and termination in modular multienzymes. *Chem. Biol.* 8, 817–829.
- (17) Pojer, F., Li, S. M., and Heide, L. (2002) Molecular cloning and sequence analysis of the clorobiocin biosynthetic gene cluster: new insights into the biosynthesis of aminocoumarin antibiotics. *Microbiology* 148, 3901–3911.
- (18) Harris, A. K., Williamson, N. R., Slater, H., Cox, A., Abbasi, S., Foulds, I., Simonsen, H. T., Leeper, F. J., and Salmond, G. P. (2004) The *Serratia* gene cluster encoding biosynthesis of the red antibiotic, prodigiosin, shows species- and strain-dependent genome context variation. *Microbiology* 150, 3547–3560.
- (19) Thomas, M. G., Burkart, M. D., and Walsh, C. T. (2002) Conversion of L-proline to pyrrolyl-2-carboxyl-S-PCP during undecylprodigiosin and pyoluteorin biosynthesis. *Chem. Biol.* 9, 171–84.
- (20) Garneau, S., Dorrestein, P. C., Kelleher, N. L., and Walsh, C. T. (2005) Characterization of the formation of the pyrrole moiety during clorobiocin and coumermycin A1 biosynthesis. *Biochemistry* 44, 2770–2780.
- (21) Garneau-Tsodikova, S., Dorrestein, P. C., Kelleher, N. L., and Walsh, C. T. (2006) Protein assembly line components in prodigiosin biosynthesis: characterization of PigA,G,H,I,J. *J. Am. Chem. Soc.* 128, 12600–12601.
- (22) Walsh, C. T., Garneau-Tsodikova, S., and Howard-Jones, A. R. (2006) Biological formation of pyrroles: nature's logic and enzymatic machinery. *Nat. Prod. Rep.* 23, 517–531.
- (23) Zhang, X., and Parry, R. J. (2007) Cloning and characterization of the pyrrolomycin biosynthetic gene clusters from *Actinosporangium vitaminophilum* ATCC 31673 and *Streptomyces* sp. strain UC 11065. *Antimicrob. Agents Chemother.* 51, 946–957.
- (24) Meiser, P., Weissman, K. J., Bode, H. B., Krug, D., Dickschat, J. S., Sandmann, A., and Müller, R. (2008) DKxanthene biosynthesis: understanding the basis for diversity-oriented synthesis in myxobacterial secondary metabolism. *Chem. Biol.* 15, 771–781.
- (25) Li, C., Roeger, K. E., and Kelly, W. L. (2009) Analysis of the indanomycin biosynthetic gene cluster from *Streptomyces antibioticus* NRRL 8167. *ChemBioChem* 10, 1064–1072.
- (26) Kopp, M., Irschik, H., Gempeler, K., Buntin, K., Meiser, P., Weissman, K. J., Bode, H. B., and Müller, R. (2011) Insights into the complex biosynthesis of the leupyrrins in *Sorangium cellulosum* So ce690. *Mol. Biosyst.* 7, 1549–1563.
- (27) Thompson, J. D., Gibson, T. J., Plewniak, F., Jeanmougin, F., and Higgins, D. G. (1997) The ClustalX windows interface: flexible strategies for multiple sequence alignment aided by quality analysis tools. *Nucleic Acids Res.* 25, 4876–4882.
- (28) Bradford, M. M. (1976) A rapid and sensitive method for the quantitation of microgram quantities of protein utilizing the principle of protein-dye binding. *Anal. Biochem.* 72, 248–254.
- (29) Fujihara, H., and Schowen, R. L. (1984) Facile, economical synthesis of L-[alpha-²H]-alpha-amino acids. *J. Org. Chem.* 49, 2819–2820.
- (30) Hamilton, P. B. (1952) Proline: synthesis from ornithine, citrulline, or arginine. *J. Biol. Chem.* 198, 587–597.
- (31) Prasad, A. S. B., Kanth, J. V. B., and Periasamy, M. (1992) Convenient methods for the reduction of amides, nitriles, carboxylic esters, acids and hydroboration of alkenes using NaBH₄/I₂ system. *Tetrahedron* 48, 4623–4628.
- (32) Oba, M., Terauchi, T., Hashimoto, J., Tanaka, T., and Nishiyama, K. (1997) Stereoselective synthesis of (2S,3S,4R,5S)-proline-3,4,5-d₃. *Tetrahedron Lett.* 38, 5515–5518.
- (33) Geoghegan, K. F., Dixon, H. B., Rosner, P. J., Hoth, L. R., Lanzetti, A. J., Borzilleri, K. A., Marr, E. S., Pezzullo, L. H., Martin, L. B., LeMotte, P. K., McColl, A. S., Kamath, A. V., and Stroh, J. G. (1999) Spontaneous alpha-N-6-phosphogluconoylation of a "His tag" in *Escherichia coli*: the cause of extra mass of 258 or 178 Da in fusion proteins. *Anal. Biochem.* 267, 169–184.
- (34) Tiffany, K. A., Roberts, D. L., Wang, M., Paschke, R., Mohsen, A. W., Vockley, J., and Kim, J. J. (1997) Structure of human isovaleryl-CoA dehydrogenase at 2.6 Å resolution: structural basis for substrate specificity. *Biochemistry* 36, 8455–8464.
- (35) Dorrestein, P. C., Bumpus, S. B., Calderone, C. T., Garneau-Tsodikova, S., Aron, Z. D., Straight, P. D., Kolter, R., Walsh, C. T., and Kelleher, N. L. (2006) Facile detection of acyl and peptidyl intermediates on thiotemplate carrier domains via phosphopantetheinyl elimination reactions during tandem mass spectrometry. *Biochemistry* 45, 12756–12766.
- (36) Dorrestein, P. C., and Kelleher, N. L. (2006) Dissecting non-ribosomal and polyketide biosynthetic machineries using electrospray ionization Fourier-Transform mass spectrometry. *Nat. Prod. Rep.* 23, 893–918.
- (37) Meluzzi, D., Zheng, W. H., Hensler, M., Nizet, V., and Dorrestein, P. C. (2008) Top-down mass spectrometry on low-resolution instruments: characterization of phosphopantetheinylated carrier domains in polyketide and non-ribosomal biosynthetic pathways. *Bioorg. Med. Chem. Lett.* 18, 3107–3111.
- (38) Ghisla, S., and Thorpe, C. (2004) Acyl-CoA dehydrogenases. A mechanistic overview. *Eur. J. Biochem.* 271, 494–508.
- (39) Kim, J. J., and Miura, R. (2004) Acyl-CoA dehydrogenases and acyl-CoA oxidases. Structural basis for mechanistic similarities and differences. *Eur. J. Biochem.* 271, 483–493.
- (40) Dakoji, S., Shin, I., Becker, D. F., Stankovich, M. T., and Liu, H. W. (1996) Studies of Acyl-CoA Dehydrogenase Catalyzed Allylic Isomerization: A One-Base or Two-Base Mechanism? *J. Am. Chem. Soc.* 118, 10971–10979.
- (41) Dakoji, S., Shin, I., Battaile, K. P., Vockley, J., and Liu, H. W. (1997) Redesigning the active-site of an acyl-CoA dehydrogenase: new evidence supporting a one-base mechanism. *Bioorg. Med. Chem.* 5, 2157–2164.
- (42) Zeng, J., and Li, D. (2005) Intrinsic isomerase activity of medium-chain acyl-CoA dehydrogenase. *Biochemistry* 44, 6715–6722.
- (43) Müller, C., Nolden, S., Gebhardt, P., Heinzmann, E., Lange, C., Puk, O., Welzel, K., Wohlleben, W., and Schwartz, D. (2007) Sequencing and analysis of the biosynthetic gene cluster of the lipopeptide antibiotic friulimycin in *Actinoplanes friuliensis*. *Antimicrob. Agents Chemother.* 51, 1028–1037.
- (44) Heinzmann, E., Berger, S., Müller, C., Hartner, T., Poralla, K., Wohlleben, W., and Schwartz, D. (2005) An acyl-CoA dehydrogenase is involved in the formation of the Delta cis3 double bond in the acyl residue of the lipopeptide antibiotic friulimycin in *Actinoplanes friuliensis*. *Microbiology* 151, 1963–1974.
- (45) Keenan, M. V., and Alworth, W. L. (1974) The inhibition of proline racemase by a transition state analogue: Delta-1-pyrroline-2-carboxylate. *Biochem. Biophys. Res. Commun.* 57, 500–504.

(46) Lewis, M. L., Martin, S. L., Rowe, C. J., Sutherland, J. D., Wilson, E. J., and Wright, M. C. (1993) Reduction of Δ -1-pyrroline-2-carboxylic acid to proline by an *Escherichia coli* proline auxotroph. *Bioorg. Med. Chem. Lett.* 3, 1189–1192.

(47) Lewis, M. L., Rowe, C. J., Sewald, N., Sutherland, J. D., Wilson, E. J., and Wright, M. C. (1993) The effect of pH on the solution structure of Δ -1-pyrroline-2-carboxylic acid as revealed by NMR and electrospray mass spectroscopy. *Bioorg. Med. Chem. Lett.* 3, 1193–1196.